Journal of Chemistry and Technologies, 2025, *33*(2), 326-332

Journal of Chemistry and Technologies

pISSN 2663-2934 (Print), ISSN 2663-2942 (Online).

journal homepage: http://chemistry.dnu.dp.ua
editorial e-mail: chem.dnu@gmail.com

UDC 665.584.01:544.252.24

GREEN SYNTHESIS OF IRON NANOPARTICLES USING BIO-WASTE EXTRACTS

Majid Ali[1], Rizwan Alam[1], Muhammad Shakeel[1], Fariha Un Nisa[2*], Kashif Ashraf[3], Syed Majid Bukhari[2*], Asma Zaidi[2]

[1]*Department of Chemistry, Government Postgraduate College No. 1, Abbottabad, Higher Education Department KP, Pakistan*
[2]*Department of Chemistry, COMSATS University Islamabad, Abbottabad Campus, 22060, KPK, Pakistan*
[3]*Mechanical Engineering Technology Department, Government Swedish Pakistani College of Technology, 50700, Gujrat, Pakistan*

Received 9 December 2025; accepted 25 February 2025; available online 15 July 2025

Abstract

Green synthesis of nanoparticles using naturally occurring biomolecules is an efficient, cost-effective, and eco-friendly procedure. In this study, the synthesis of iron nanoparticles is reported by using aqueous extracts of almond seed skin, grape seeds, and pomegranate peels. These extracts work as reducing, stabilizing, and capping agents. In aqueous extracts of each sample, 0.1 M iron sulfate solution was added drop-wise which turned the color of the solution to black. This indicated the successful synthesis of iron nanoparticles. The synthesized nanoparticles were extracted from their respective colloidal solutions by centrifugation and characterized by suitable characterization techniques including SEM, UV-visible, and FT-IR spectroscopy. UV-visible spectra of iron nanoparticles showed significant differences from the extracts and from the iron sulfate solution. This indicated the successful synthesis of iron nanoparticles and their surface capping with biomolecules. The SEM micrograph revealed that the shape of nanoparticles was spherical; The average sizes of grape seeds extract, almond skins extract, and pomegranate peels extract iron nanoparticles were 72.95±3.28 nm, 79.31±2.37 nm, and 77.19±1.84 nm diameter, respectively. The FT-IR spectroscopic study revealed that the most probable compounds involved in the capping and stabilizing of the nanoparticles are phenols/polyphenols, carboxylic acid derivatives, amino acids, and aliphatic/aromatic amines. These iron nanoparticles coated with biomolecules may be further analyzed for their anti-oxidant and anti-cancer activity.

Keywords: almond seed skin; pomegranate peels; grape seeds; Scanning Electron Microscopy; FT-IR spectroscopy.

ЗЕЛЕНИЙ СИНТЕЗ НАНОЧАСТИНОК ЗАЛІЗА З ВИКОРИСТАННЯМ ЕКСТРАКТІВ БІОВІДХОДІВ

Маджид Алі[1], Різван Алам[1], Мухаммед Шакіл[1], Фаріха Ун Ніса[2*], Кашиф Ашраф[3], Саїд Маджид Бухарі[2*], Асма Заїді[2]

[1]*Державний коледж післядипломної освіти № 1, Абботтабад, Департамент вищої освіти КП, Пакистан*
[2]*Університет COMSATS Ісламабад, кампус Абботтабад, 22060, ХПК, Пакистан*
[3]*Державний шведський пакистанський технологічний коледж, 50700, Гуджрат, Пакистан*

Анотація

Екологічно чистий синтез наночастинок з використанням природних біомолекул є ефективною, економічно вигідною та екологічно чистою процедурою. У цьому дослідженні описано синтез наночастинок заліза з використанням водних екстрактів шкірки мигдалевого насіння, виноградних кісточок і гранатової шкірки. Ці екстракти діють як відновлювачі, стабілізатори та капсульовані агенти. До водних екстрактів кожного зразка додавали по краплях 0.1 М розчин залізного купоросу, який забарвлював розчин у чорний колір. Це свідчило про успішний синтез наночастинок заліза. Синтезовані наночастинки були виділені з відповідних колоїдних розчинів центрифугуванням і охарактеризовані за допомогою відповідних методів, включаючи СЕМ, УФ- та ІЧ-спектроскопію. УФ-спектри наночастинок заліза показали значні відмінності від екстрактів та розчину сульфату заліза. Це свідчить про успішний синтез наночастинок заліза та покриття їх поверхні біомолекулами. SEM-мікрофотографія показала, що форма наночастинок була сферичною; середній розмір наночастинок заліза з екстракту виноградних кісточок, екстракту мигдальної шкірки та екстракту шкірки граната становив 72.95±3.28 нм, 79.31±2.37 нм та 77.19±1.84 нм в діаметрі, відповідно. ІЧ-спектроскопічне дослідження показало, що найбільш ймовірними сполуками, які беруть участь у покритті та стабілізації наночастинок, є феноли/поліфеноли, похідні карбонових кислот, амінокислоти та аліфатичні/ароматичні аміни. Ці наночастинки заліза, вкриті біомолекулами, можуть бути додатково проаналізовані на предмет їхньої антиоксидантної та протиракової активності.

Ключові слова: шкірка мигдалевих кісточок; гранатові кірки; виноградні кісточки; растрова електронна мікроскопія; ІЧ-спектроскопія; Фур'є-спектроскопія.

**Corresponding author: e-mail: fariharasheed557@gmail.com; majidbukhari@cuiatd.edu.pk*

Journal of Chemistry and Technologies, 2025, *33*(2), 326-332

Introduction

The wide range of characteristics of metal oxides along with the exceptional properties of their nanoparticles (NPs) are the center of attention for researchers. These inorganic solids are being extensively explored these days. The applications of transition metal oxides in industry have been reported recently; such molecules play a substantial part in environmental remediation and medication. Due to these extensive applications, metal oxide NPs are being focused upon currently in the field of nanoscience and nanotechnology [1].

To obtain a variety in morphologies and sizes, several schemes of synthesis including hydrothermal method, vapor deposition method, seed-mediated technique, microwave-assisted synthesis, spray pyrolysis, and wet chemical approach were used to prepare metal oxide NPs [1; 2]. However, the research interest of scientists has shifted from conservative synthetic routes to biosynthetic approaches where microorganisms or biowastes could be employed for synthesizing the NPs. Various molecules and surfactants may act as capping agents to impart useful characteristics to the NPs in terms of their shapes, sizes, and surfaces thereby preventing aggregation [1–5]. Biological compounds of natural origin have been recognized to actively participate in the synthesis of NPs with numerous shapes and sizes [2]. Utilizing waste products in this regard proves to be dually beneficial in terms of cost minimization, making the synthetic route cost-effective and limiting the requirement of hazardous chemicals for synthesis; therefore, stimulating "green synthesis" [6]. The biological potential of these organic compounds is proven against cancerous situations, diabetes, thrombosis, obesity, and other progressive diseases; these compounds perform their role as reducing and capping agents [3–9].

Iron-oxide NPs belong to a vital classification of NPs, which possess many applications in different fields of science due to their unique properties [2; 4]. According to the literature, the polysaccharides found in the water extract of *Sargassum muticum* helped to reduce the ferric chloride solution. This process resulted in the creation of ferric oxide (Fe_3O_4) NPs which were cubic from a morphological aspect and their mean diameter was 18 ± 4 nm [3]. In another work, tea waste was used to produce magnetic iron oxide (Fe_3O_4) NPs having 5 nm to 25 nm size and (pyramid) cuboid morphology [5–8]. Samarawickrama et al. investigated the green synthesis of FeNPs using an aqueous extract of *Murraya koenigii* leaves where they focused on the synthesis mechanism, characterization, and antibacterial activity of FeNPs [10]. Similarly, Tyagi et al. reported the green synthesis of FeNPs from spinach leaf and banana peel aqueous extracts and evaluated their antibacterial potential [11]. Ardakani et al. reported the green synthesis of iron-based NPs using *Chlorophytum comosum* leaf extract highlighting their effectiveness in methyl orange dye degradation and antimicrobial properties [12]. Similarly, Buraki et al. explored the green synthesis of iron oxide NPs using *Hibiscus rosa-sinensis* flowers and assessed their antibacterial activity [13].

The aim of this research project is to develop NPs that can effectively purify aqueous samples [5–8].

Results and discussion

Synthesis of Iron nanoparticles. Aqueous extracts of almond skins, grape seeds, and pomegranate peels were obtained, as shown in Figure 1 (a). Following the dropwise addition of 0.1 M iron sulfate solution into the extracts, the color of each solution changed from reddish-brown to black, indicating the successful synthesis of FeNPs, as shown in Figure 1 (b). Numerous studies have reported the green synthesis of FeNPs, commonly characterized by a color change to black, confirming the formation of required NPs [10-11, 14]. Biomolecules present in the extracts might have played an important role as reducing and capping agents [6-8, 14]. The synthesized NPs were collected from their colloidal solutions through centrifugation, as shown in Figure 1 (c). After the removal of nanoparticles, the color of the solutions becomes transparent (Figure 1 (d)).

Characterization of iron nanoparticles. After the reaction with iron sulfate solution, the change in color of each extract was quantified by taking UV-Vis spectra in the range of 200–500 nm. The spectra of all the extracts before the reaction exhibited two larger and broader bands in the range of 230–295 nm, as shown in black lines in Figure 2 (a), (b), (c). The literature survey shows that these bands presumably correspond to phenolic compounds, flavanols anthocyanins, etc. [7]. Therefore, it can safely be stated that the synthesized FeNPs are rich in these classes of compounds. Another larger band at 385 nm was observed in the case of pomegranate peels (PP) extract, as shown in Figure 2 (c), whereas very small bands at 400 nm were observed in the case of almond skin (AS) and grape seeds (GS) extracts,

Journal of Chemistry and Technologies, 2025, *33*(2), 326-332

shown in Figure 2 (a) and (b), respectively. These signals showed enhancement and shift of 5 nm – 15 nm towards the longer wavelength after the reaction with iron sulfate solution.

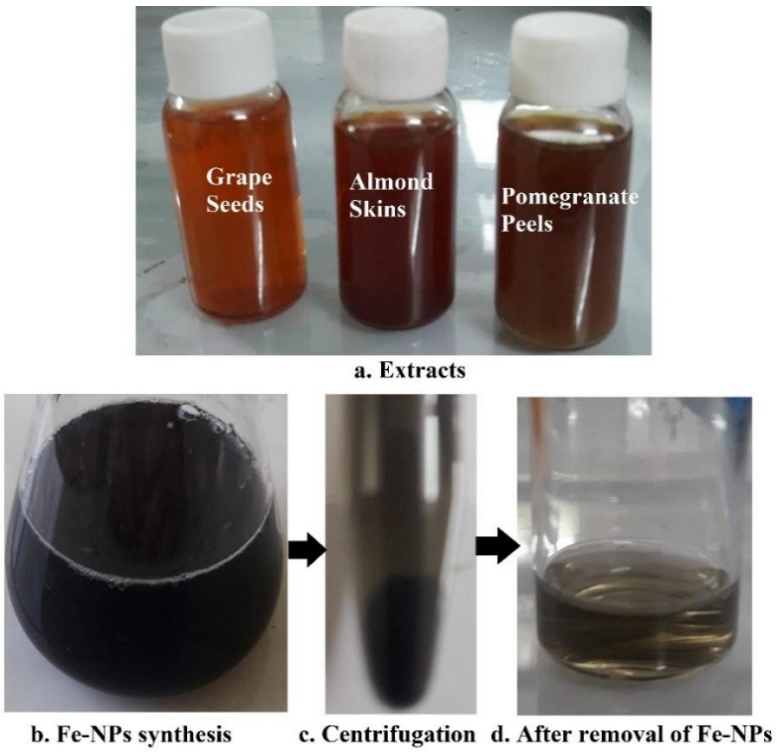

Fig. 1. (a) Aqueous extracts of grape seeds, almond seed skins, and pomegranate peels; (b) Synthesized FeNPs after reaction with iron sulfate solution; (c) centrifugation for extraction of FeNPs; (d) Color of solution after removal of FeNPs

Particularly, in the case of almond skin extract FeNPs (AS. FeNPs), the band at 230 nm shifted towards 245 nm, and the band at 280 nm to 295 nm, as shown by the red line in Figure 2 (a). In the case of grape seeds extract FeNPs (GS. FeNPs) the band at 240 nm shifted to 245 nm and the signal at 280 nm moved to 295 nm, as shown by the red line in Figure 2 (b). Whereas, in the case of pomegranate peel extract FeNPs (PP. FeNPs) both bands in the extract were already present at 245 nm and 295 nm, therefore they retained their positions but the signals appearing at 385 nm showed enhancement and shift to 400 nm, as shown by the red line in Figure 2 (c). Samarawickrama et al. observed a UV-Vis absorption signal in the case of FeNPs synthesized from the aqueous extract of *Murraya koenigii* leaves within the range of 240-310 nm [10]. Similarly, Tyagi et al. reported a UV-Vis spectra for spinach- and banana-derived FeNPs showing signals at 240 nm, 270 nm, and 395 nm [11]. These findings in the literature are consistent with the results presented in this study and further support the results obtained in our case. After removal of FeNPs from these extracts, the bands either faded again and shifted towards shorter wavelengths or completely disappeared, as shown by the green lines in Figure 2 (a), (b), (c), which indicates that the associated biomolecules present in the extracts were utilized for the synthesis of FeNPs. Similar studies have been reported which confirm the results obtained in the present [6–8, 15].

The UV-Vis spectra of FeNPs obtained from almonds, grapes, and pomegranates, were found to be almost similar and had characteristic bands at 245 nm, 295 nm, and 400 nm, as shown in Figure 2 (d). When comparing the results with the spectrum of iron sulfate solution, it was observed that the signal at 225 nm boosted and shifted to 245 nm, whereas, the signal at 295 nm remained at the same position but enhanced expressively. However, a new signal at 400 nm was also observed in the spectra of FeNPs. Thus, the spectra of FeNPs possessed significant differences from the parent extracts and iron sulfate solution, indicating successful synthesis of FeNPs and their surface capping with biomolecules.

Journal of Chemistry and Technologies, 2025, *33*(2), 326-332

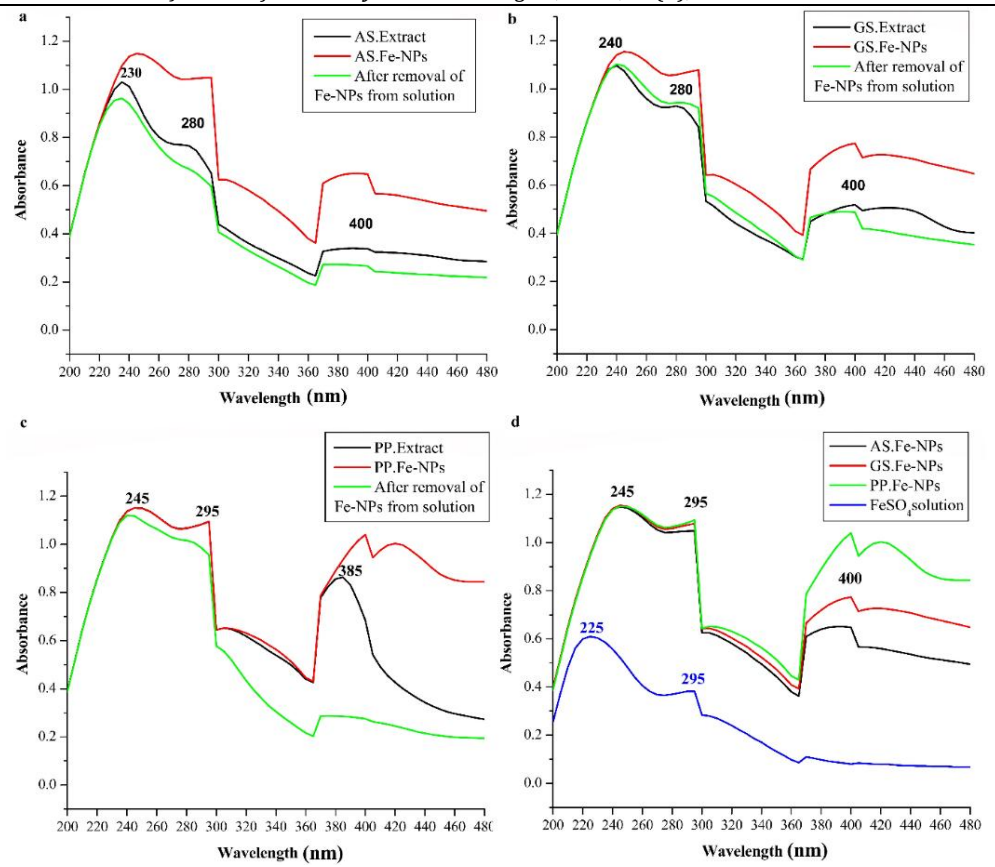

Fig. 2. UV-Vis spectra of aqueous extracts (black lines), synthesized FeNPs (red lines), and after removal of FeNPs (green lines); (a) from almond seed skins; (b) from grape seeds; (c) from pomegranate peels; (d) comparison of spectra of FeNPs with each other and iron sulfate solution (blue line)

Morphology and size distribution of FeNPs synthesized from grapes seeds extract (GS. FeNPs), almond skins extract (AS. FeNPs) and pomegranate peels extract (PP. FeNPs), were characterized using Scanning Electron Microscopy (SEM), as shown in Figure 3 (a), (b) and (c), respectively. Micrographs of all three types of FeNPs confirmed the successful synthesis of spherical shape nanoparticles. Arrows in the figure indicating different nanoparticles highlight their spherical shape.

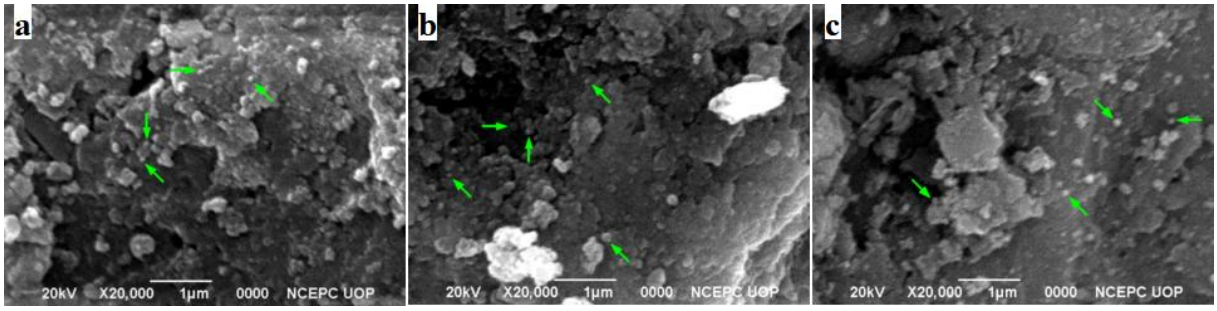

Fig. 3. SEM micrograph of FeNPs; (a) from grape seeds extract; (b) from almond seed skins extract; (c) from pomegranate peels extract

The sizes were measured using Image J software [16], with twenty readings taken from each image. The data was then analyzed using OriginPro software with the Gauss-Fit tool. The average sizes of grape seeds extract, almond skins extract, and pomegranate peels extract FeNPs were 72.95±3.28 nm, 79.31±2.37 nm, and 77.19±1.84 nm diameter, respectively, as shown in Figure 4 (a), (b) and (c).

Journal of Chemistry and Technologies, 2025, *33*(2), 326-332

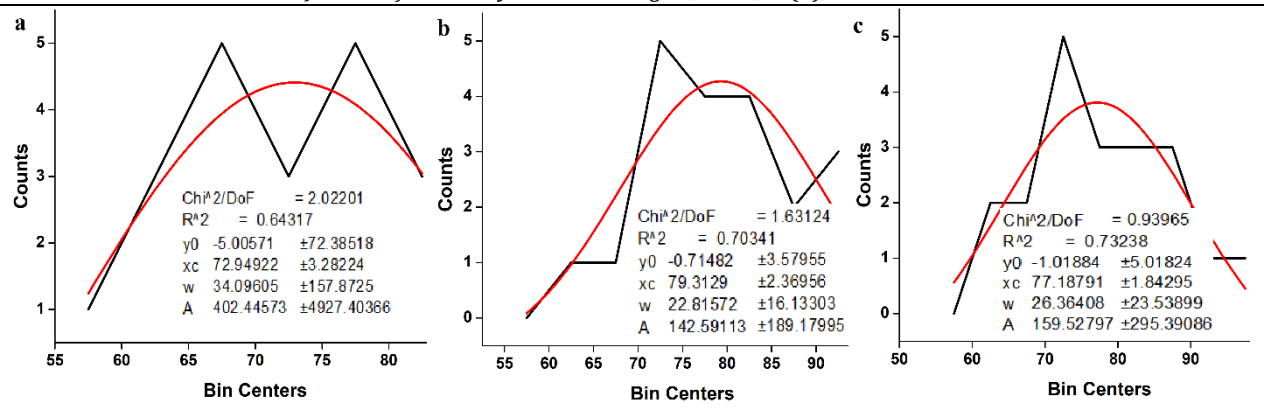

Fig. 4. Statistical data analysis for particle size determination of (a) Grape Seeds extract FeNPs (b) almond skins extract FeNPs (c) pomegranate peels extract FeNPs, through OriginPro software by applying Gauss-Fit tool

Gupta et al. analyzed the morphology of FeNPs using SEM and TEM, revealing their spherical shape with a particle size range of 30–70 nm [14]. Similarly, Samarawickrama et al. recently reported the size of FeNPs in the nanoscale range, exhibiting a spherical shape [10]. Another study reported the synthesis of spherical shape FeNPs with an average size of 36 nm using rooibos tea extract [17]. All these studies are consistent with our findings and comparison with them supports the results of this study.

The FT-IR spectra of (AS. FeNPs), (GS. FeNPs), and (PP. FeNPs), and their extracts before the reaction, were recorded and presented in Figure 5 (a), (b), and (c). A significant difference was observed when the FT-IR spectra of NPs were compared with their original extracts, as shown in Figure 5. The appearance of well-defined signals at 466 cm^{-1} and 617 cm^{-1} in the case of GS. FeNPs (Figure 5 a), 466.7 cm^{-1} and 607 cm^{-1} in PP. FeNPs (Figure 5 b), and 467 cm^{-1}, 546 cm^{-1}, and 606 cm^{-1} in case of AS. FeNPs (Figure 5 c) confirmed the synthesis of FeNPs. The results were compared with the research data, which were in agreement with the literature [7; 15].

The FT-IR spectra provide information about possible biomolecules present on the surface of FeNPs [6; 7]. The spectra revealed that all three types of FeNPs were almost similar, as shown in Figure 5 (d). Compared to previously published data, signals obtained at 3620 cm^{-1} and 3160 cm^{-1} correspond to the -OH stretching vibrations of hydroxyl groups, signals at 3520 cm^{-1} and 3300 cm^{-1} are due to -NH stretching vibrations of primary aliphatic amines, signal at 1556 cm^{-1} corresponds to the amide II linkage, mainly associated with -NH- bending vibrations and -CN- stretching vibrations, whereas the signal at 1660 cm^{-1} corresponds to amide I linkage due to stretching vibration of -CO- group [6–8; 18; 19]. In the case of PP. FeNPs the band at 1710 cm^{-1} corresponds to the -CO- stretching vibrations of the carboxylic group, the band at 1425 cm^{-1} corresponds to -OH bending of carboxylic acid functional group, band at 1345 cm^{-1} correlates with C-N stretching mode of aromatic amine and signal at 1075 cm^{-1} corresponds to C-O-C stretching and -OH bending vibrations of phenols. These findings are consistent with the data in the literature[6–8; 18]. Thus, the FT-IR spectroscopic study revealed that the most probable compounds involved in the capping and stabilization of NPs are phenols/polyphenols, carboxylic acids and their derivatives, amino acids, aliphatic and aromatic amines.

Experiment

Preparation of the extracts. Analytical grade iron sulfate ($FeSO_4$) was purchased from Sigma-Aldrich. All solutions were prepared in deionized water. Fresh almonds, grapes, and pomegranates were purchased from the local market in Abbottabad, Pakistan. Almond seeds were soaked in deionized water for 3-4 hours and their skins were peeled off and dried in an oven at 70 °C for 1 hour, as reported by Pan Z et al., (2020) [7]. Grape seeds and pomegranate peels were washed with deionized water and dried in an oven at 70 °C for 4 hours. Each of these was ground into powdered form in a homogenizer. An aqueous extract of each of these i.e. almond seed skins, grape seeds, and pomegranate peels, was prepared by boiling 2 g powder of each in 200 ml of deionized water until the final volume reached 100 ml [7]. Thereafter, solid residue was removed by filtration, and extracts were stored at 4 ^{0}C following the methodology adopted by Ismail E. H et al., (2014) [8].

Journal of Chemistry and Technologies, 2025, *33*(2), 326-332

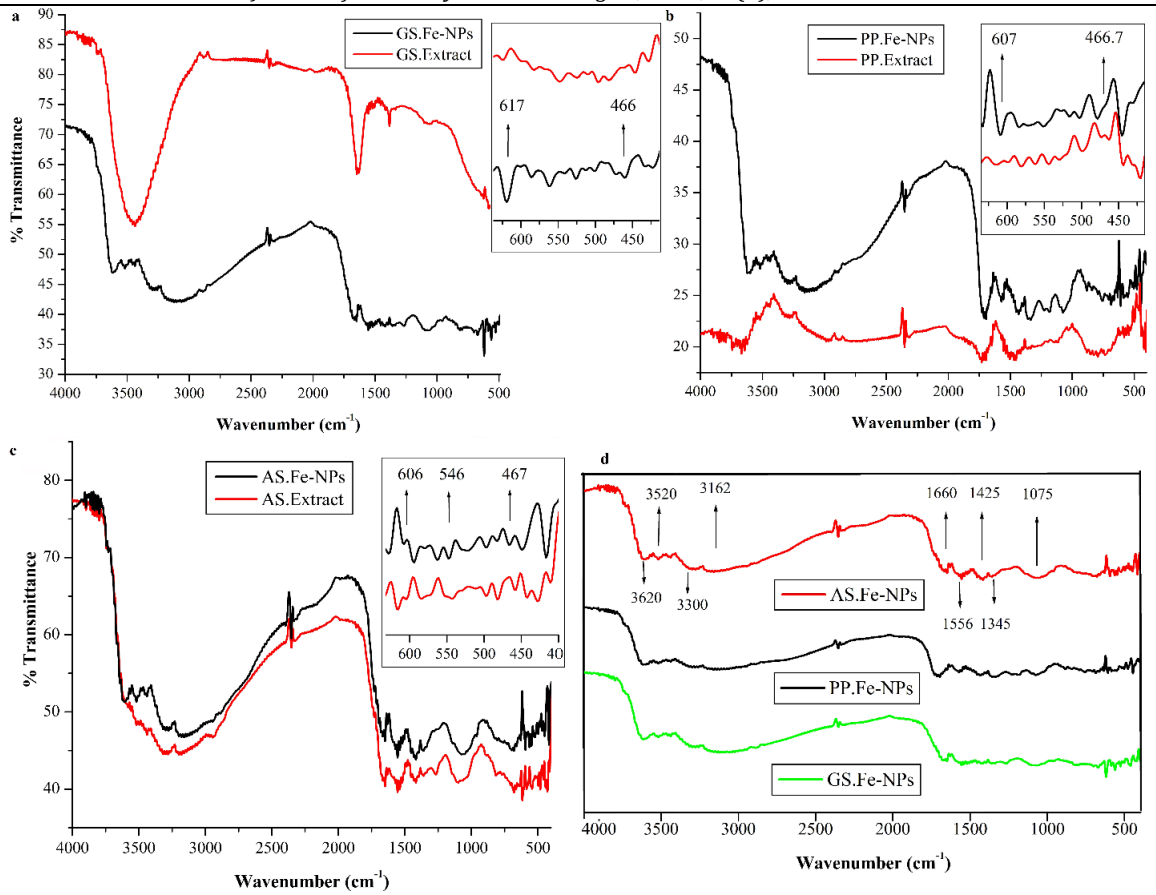

Fig. 5. The FT-IR spectra of (a) grape seed extracts and their FeNPs; (b) pomegranate peels extract and their FeNPs; (c) almond seed skins extract and their FeNPs; (d) comparison of FeNPs of all three extracts and their FT-IR signals

*Synthesis of iron nanoparticles***.** Iron sulfate ($FeSO_4$) solution of 0.1 M, was added dropwise in 100 ml solution of each (almond seed skins, grape seeds, and pomegranate peels) extract, with constant stirring at room temperature, until the color of the solution turned black, indicating the synthesis of FeNPs, as reported previously by Pan Z et al., (2020) [6; 7]. Extraction of NPs from the colloidal solution was carried out by centrifugation at 14000 rpm for 15 minutes, washed with distilled water, and dried in open air according to the described procedure [8]. *Characterization of iron nanoparticles.* The Morphology and size distribution of FeNPs were obtained by field emission Scanning Electron Microscopy (SEM) at different magnifications with an accelerating voltage of 20 kV. The data were analyzed using ImageJ software, and statistical analysis was performed using OriginPro Software. The UV-visible spectra of the extracts, before and after the reaction with iron sulfate ($FeSO_4$) solution, were recorded. Fourier transform infrared spectra (FT-IR) of extracts and synthesized FeNPs were obtained to analyze the surface of nanoparticles. The FT-IR spectra were recorded using a Thermo Nicolet iS50-6700 FT-IR spectrophotometer (Vienna, Austria). The instrument is ATR, which allows the direct sample application. Therefore, the samples were directly placed on the dock (sample compartment). No sample disc preparation was necessary in this process. The associated software in the computer setup connected to the instrument was used to set the wavenumber range, and the sample spectrum in each case was recorded after baseline correction by giving commands to the computer software.

Conclusion

We synthesized iron nanoparticles from aqueous extracts of almond seed skins, grape seeds, and pomegranate peels without using any reducing agents. Biomolecules present in the extracts might have played an important role in capping and reducing agents. The SEM micrograph revealed the successful synthesis of spherical shape iron nanoparticles with diameters of 72.95±3.28 nm for grape seeds extract, 79.31±2.37 nm for almond skins extract, and 77.19±1.84 nm for pomegranates peels extract. The FT-IR spectroscopic study revealed that the most probable compounds involved in the capping and stabilization of nanoparticles are phenols/polyphenols, carboxylic acids and their

derivatives, amino acids, and aliphatic/aromatic amines.

In the future, these iron nanoparticles may be studied further as anti-cancer agents, adsorption, and catalysis.

Acknowledgements

We acknowledge the Higher Education Department KP, Pakistan for providing us necessary facilities.

Conflict of interest

No conflict of interest.

References

[1] Sharma, D., Kanchi, S., Bisetty, K. (2019). Biogenic synthesis of nanoparticles: A review. *Arabian Journal of Chemistry, 12*(8), 3576–3600. doi.org/10.1016/j.arabjc.2015.11.002

[2] Herlekar, M., Barve, S., Kumar, R. (2014). Plant-mediated green synthesis of iron nanoparticles. *Journal of Nanoparticles, 2014*, 140614. doi.org/10.1155/2014/140614

[3] Mahdavi, M., Namvar, F., Ahmad, M.B., Mohammad, R. (2013). Green biosynthesis and characterization of magnetic iron oxide (Fe_3O_4) nanoparticles using seaweed (Sargassum muticum) aqueous extract. *Molecules*, *18*(5), 5954–5964. doi: 10.3390/molecules18055954

[4] Magnacca, G., Allera, A., Montoneri, E., Celi, L., Benito, D.E., Gagliardi, L.G., Gonzalez, M.C., Mártire, D.O., Carlos, L. (2014). Novel magnetite nanoparticles coated with waste-sourced biobased substances as sustainable and renewable adsorbing materials. *ACS Sustainable Chemistry & Engineering*, *2*(6), 1518–1524. doi.org/10.1021/sc500213j

[5] Lunge, S., Singh, S., Sinha, A. (2014). Magnetic iron oxide (Fe_3O_4) nanoparticles from tea waste for arsenic removal. *Journal of Magnetism and Magnetic Materials*, *356*, 21–31. doi.org/10.1016/j.jmmm.2013.12.008

[6] Gao, J.-F., Li, H.-Y., Pan, K.-L., Si, C.-Y. (2016). Green synthesis of nanoscale zero-valent iron using a grape seed extract as a stabilizing agent and the application for quick decolorization of azo and anthraquinone dyes. *RSC Advances*, *6*(27), 22526–22537. doi.org/10.1039/C5RA26668H

[7] Pan, Z., Lin, Y., Sarkar, B., Owens, G., Chen, Z. (2020). Green synthesis of iron nanoparticles using red peanut skin extract: Synthesis mechanism, characterization and effect of conditions on chromium removal. *Journal of Colloid and Interface Science*, *558*, 106–114. doi.org/10.1016/j.jcis.2019.09.106

[8] Ismail, E.H., Khalil, M.M.H., Seif, F.A.A., El-Magdoub, F. (2014). Biosynthesis of gold nanoparticles using extract of grape (Vitis Vinifera) leaves and seeds. *Progress in Nanotechnology and Nanomaterials*, *3*(1), 1–12.

[9] Arif, A., Bhatti, A., John, P. (2019). Therapeutic potential of Foeniculum vulgare mill. Derived selenium nanoparticles in arthritic Balb/c mice. *International Journal of Nanomedicine*, *14*, 8561–8572. doi: 10.2147/IJN.S226674.

[10] Samarawickrama, R., Wijayapala, S., Fernando, A.N. (2024). Green synthesis of iron nanoparticles (FeNPs) using aqueous extract of *Murraya koenigii* leaves: synthesis mechanism, characterization process and antibacterial activity. *Nanoscience & Nanotechnology-Asia, 14*, e22106812320014. doi: 10.2174/0122106812320014240823184253

[11] Tyagi, P.K., Gupta, S., Tyagi, S., Kumar, M., Pandiselvam, R., Daştan, S.D., Sharifi-Rad, J., Gola, D., Arya, A. (2021). Green synthesis of iron nanoparticles from spinach leaf and banana peel aqueous extracts and evaluation of antibacterial potential. *Journal of nanomaterials, 2021*(1), 4871453. doi.org/10.1155/2021/4871453

[12] Ardakani, L.S., Alimardani, V., Tamaddon, A.M., Amani, A.,M., Taghizadeh, S. (2021). Green synthesis of iron-based nanoparticles using Chlorophytum comosum leaf extract: methyl orange dye degradation and antimicrobial properties. *Heliyon, 7*(2), e06159. doi.org/10.1016/j.heliyon.2021.e06159

[13] Buarki, F., AbuHassan, H., Al-Hannan, F., Henari, F.Z. (2022). Green synthesis of iron oxide nanoparticles using Hibiscus rosa sinensis flowers and their antibacterial activity. *Journal of Nanotechnology, 2022*(1), 5474645. doi.org/10.1155/2022/5474645

[14] Gupta, K., Saini, K., Mathur, J. (2023). Eco-Friendly Synthesis of Iron Nanoparticles Using Green Tea Extract: Characterization and Evaluation of Their Catalytic, Anti-oxidant and Anti-bacterial Potentials. *Chemistry Select, 8*(13), e202204421. doi.org/10.1002/slct.202204421

[15] Jin, X., Liu, Y., Tan, J., Owens, G., Chen, Z. (2018). Removal of Cr(VI) from aqueous solutions via reduction and absorption by green synthesized iron nanoparticles. *Journal of Cleaner Production, 176*, 929–936. doi.org/10.1016/j.jclepro.2017.12.026

[16] Schneider, C. A., Rasband, W.S., Eliceiri, K.W. (2012). NIH Image to ImageJ: 25 years of image analysis. *Nature Methods*, *9*, 671–675. doi.org/10.1038/nmeth.2089

[17] Kimpiab, E., Kapiamba, K.F., Folifac, L., Oyekola, O., Petrik, L. (2022). Synthesis of stabilized iron nanoparticles from acid mine drainage and rooibos tea for application as a Fenton-like catalyst. *ACS omega,* 7(28), 24423–24431. doi.org/10.1021/acsomega.2c01846

[18] Manoharan, R., Baraga, J.J., Rava, R.P., Dasari, R.R., Fitzmaurice, M., Feld, M.S. (1993). Biochemical analysis and mapping of atherosclerotic human artery using FT-IR microspectroscopy. *Atherosclerosis, 103*(2), 181–193. doi: 10.1016/0021-9150(93)90261-r

[19] Sravanthi, K., Ayodhya, D., Swamy, P.Y. (2018). Green synthesis, characterization of biomaterial-supported zero-valent iron nanoparticles for contaminated water treatment. *Journal of Analytical Science and Technology, 9*, 3(2018). doi.org/10.1186/s40543-017-0134-9.